Journal of
Materials Chemistry C

RSCPublishing

PAPER

View Article Online
View Journal | View Issue

Cite this: *J. Mater. Chem. C*, 2013, **1**, 2028

Solid-state fluorescence properties and reversible piezochromic luminescence of aggregation-induced emission-active 9,10-bis[(9,9-dialkylfluorene-2-yl)vinyl] anthracenes

Lingyu Bu, Mingxiao Sun, Deteng Zhang, Wei Liu, Yalong Wang, Meng Zheng, Shanfeng Xue and Wenjun Yang*

Received 3rd January 2013
Accepted 21st January 2013

DOI: 10.1039/c3tc00017f

www.rsc.org/MaterialsC

In this work, we have synthesized 9,10-bis[(9,9-dialkylfluorene-2-yl)vinyl]anthracene derivatives (**FLA-C*n***) with propyl, pentyl, and dodecyl side chains to investigate their fluorescence properties. The results show that **FLA-C*n*** exhibit not only an aggregation-induced emission effect but also reversible piezofluorochromic (PFC) behaviour. Interestingly, the fluorescence emission and grinding-induced spectral shifts ($\Delta\lambda_{PFC}$) of **FLA-C*n*** solids are alkyl length-dependent: the longer alkyl-containing **FLA-C*n*** solids show more blue-shifted emission and larger $\Delta\lambda_{PFC}$. Moreover, the fluorescence emission of ground **FLA-C12** solid can recover spontaneously at room temperature, Powder wide-angle X-ray diffraction and differential scanning calorimetry experiments reveal that the transformation between crystalline and amorphous states under various external stimuli is responsible for the PFC behaviour, and the spontaneous recovering emission of amorphized **FLA-C12** solid is ascribed to its low cold-crystallization temperature. This work demonstrates once again the accessibility of tuning the solid-state optical properties of organic fluorophores by combining the simple alternation of molecular chemical structure and the physical change of aggregate morphology under external stimuli.

Introduction

Stimuli-responsive materials, especially piezo- or mechano-fluorochromic (PFC) materials, have attracted much attention due to their potential applications in optical recording and fluorescence sensors.[1–3] In principle, changes in the solid-state fluorescence of conjugated organic materials could be achieved by chemical or physical methods. The chemical method involves solid-state chemical reactions that provoke chemical structural changes of molecules[4] and are usually incomplete and irreversible. The physical method, which involves the change of molecular packing mode instead of chemical alteration of the molecular structure, has been attracting considerable interest because switching and tuning the solid-state color and/or luminescence properties by controlling the molecular packing mode could not only provide practical applications in optical recording and sensing but also profit the fundamental understanding of photophysical properties. While there have been a variety of reports on organic and organometallic chromophores with PFC behaviour,[1–3,5–8] recently, some conjugated organic molecules exhibiting aggregation-induced/crystallization-enhanced emission (AIE/CEE) have been the new mainstay of PFC materials.[9–13] The common structural characteristics of AIE molecules are the strongly twisted skeleton conformations,[14,15] which could hinder solid-state intermolecular close stacking and intense π–π interaction and might result in these materials possessing mechanical stress-dependent stable and metastable solid morphologies that show different optical and optoelectronic properties. However, PFC materials are still at the initial stages of investigation, and the kinds of PFC materials and in-depth understanding of PFC phenomena are limited. Therefore, there is still a great demand on exploitation of new PFC materials and accumulation of knowledge of their structure–property relationships. In this context, the design and synthesis of new PFC materials with comparable molecular structures and the investigation of PFC behaviour are very interesting but scarce.

Very recently, it was reported that 9,10-bis(*p*-alkoxystyryl) anthracences only with sufficient long alkyl chains (decyl, undecyl and dodecyl) are effective PFC materials;[10i] in contrast, the shorter alkyl-containing 9,10-bis[(*N*-alkylcarbazol-3-yl)vinyl] anthracenes show more remarkable PFC behaviour.[13] These two forms of chain length-dependent PFC behaviour underline not only the complexity of the structure–property relationship of PFC materials but also the significant effect of the nature of

---

Key Laboratory of Rubber-Plastics of Ministry of Education/Shandong Provincial Key Laboratory of Rubber-Plastics, School of Polymer Science and Engineering, Qingdao University of Science & Technology, 53 Zhengzhou Road, Qingdao 266042, China. E-mail: ywjph2004@qust.edu.cn

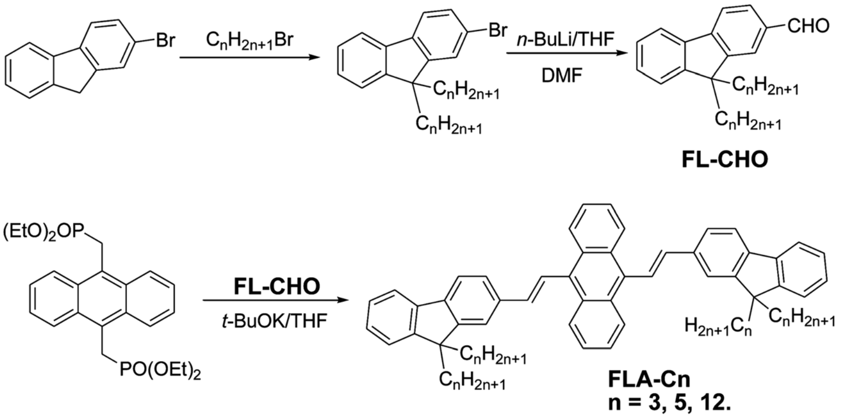

Scheme 1 Synthesis and structure of **FLA-C*n***.

end-arylenes and substituents at the aryl rings on the solid-state fluorescence and piezochromic luminescence of 9,10-bis(arylvinyl)anthracene derivatives. To further understand this phenomenon and develop new PFC materials, in the current work, we have designed and synthesized some AIE-active 9,10-bis[(9,9-dialkylfluorene-2-yl)vinyl]anthracenes with propyl, pentyl and dodecyl as side alkyl chains (**FLA-C*n***, Scheme 1) to investigate their fluorescence properties. We report here that **FLA-C*n*** not only exhibit chain length-dependent PFC behaviour, in that longer alkyl-containing **FLA-C*n*** show larger spectral shifts, but also the fluorescence color and emission of ground **FLA-C12** solid can recover spontaneously at room temperature.

Experimental section

Regents and solvents

All the chemicals were purchased from Aldrich Chemical Co. Other solvents and reagents were analytical grade and used as received, unless otherwise stated. Tetrahydrofuran (THF) was distilled over metallic sodium and dimethyl formamide (DMF) over calcium hydride before use.

Measurements

^{1}H and ^{13}C NMR spectra were recorded on a Bruker-AC500 (500 MHz) spectrometer with $CDCl_3$ as solvent and tetramethylsilane (TMS) as the internal standard. Elemental analysis was performed on a Perkin-Elmer 2400. UV-vis absorption and diffuse reflectance absorption spectra were recorded on a Hitachi U-4100 spectrophotometer. Fluorescence measurements were carried out with a Hitachi F-4600 spectrophotometer. The peak wavelength of the lowest energy absorption band was used as the excitation wavelength for the PL measurement. The fluorescence quantum yield (Φ) was determined at room temperature by the dilution method using fluorescein in water (pH = 11) as the reference. Powder wide-angle X-ray diffraction (PXD) experiments were performed on a powder X-ray diffractometer (INCA Energy, Oxford Instruments) operating at 3 kW. Differential scanning calorimetry (DSC) curves were determined on a Netzsch DSC 204F1 at a heating rate of 10 °C min^{-1}.

Piezofluorochromic and stimulus-recovering experiments

Pressing experiment: a quantity of **FLA-C*n*** and KBr powder was simply mixed in a mortar and then pressed with an IR pellet press under a pressure of 1500 psi for 1 min at room temperature. Annealing experiment: the pressed sample was put into an oven whose temperature was 20 °C over T_c (T_c is the cold-crystallization temperature of each compound) for 3 min. Solvent-fuming experiment: the pressed sample was put above the dichloromethane level and exposed to the vapor for 1 min at room temperature. Grinding experiment: at room temperature, pristine **FLA-C12** solid was put on a glass plate and ground with a metal spatula and then allowed to stand for a given time.

Synthesis

9,10-Bis(chloromethyl)anthracene. To a stirred mixture of anthracene (1.78 g, 10 mmol), anhydrous $ZnCl_2$ (1.64 g, 12 mmol), and paraformaldehyde (1.50 g, 50 mmol) in dioxane (20 mL) was slowly added concentrated aqueous hydrochloric acid (40 mL) at room temperature. The mixture was gentle refluxed for 3 h and allowed to stand for 16 h at room temperature. The resulting fine granular solid was separated by filtration and washed with H_2O and dioxane to afford the crude product. The crude product was recrystallized from toluene to give a yellowish solid (1.81 g, 64.1%). ^{1}H NMR (500 MHz, $CDCl_3$): δ 8.40 (m, 4H), 7.62 (m, 4H), 5.61 ppm (s, 4H).

9,10-Bis(diethoxylphosphorylmethyl)anthracene. A mixture of 9,10-bis(chloromethyl)anthracene (7.80 g, 28.3 mmol) and triethyl phosphite (50 mL) was stirred and gently refluxed overnight. The excess triethyl phosphite was removed by distillation under reduced pressure. The crude product was separated by silica gel column chromatography using ethyl acetate/petroleum ether (1/1, v/v) as the eluent. A yellow solid was obtained (10.4 g, 76.8%). ^{1}H NMR (500 MHz, $CDCl_3$): δ 8.32 (d, 4H), 7.53 (d, 4H), 4.21 (q, 8H), 3.78 (d, 4H), 1.11 ppm (t, 12H).

2-Bromo-9,9-didodecylfluorene. To a mixture of 50% aqueous NaOH (12 mL), DMSO (40 mL) and 2-bromofluorene (2.1 g, 8.2 mmol) was slowly added 1-bromododecane (4.9 mL, 19.6 mmol) at room temperature. The mixture was stirred at

90 °C overnight and then cooled to room temperature. After that, the mixture was added to brine and extracted with dichloromethane. The organic phase was dried over $MgSO_4$ and the solvent was removed. The residue was purified with column chromatography (silica gel, petroleum ether) to give 3.55 g of yellow liquid (75% yield). ^1H NMR (500 MHz, $CDCl_3$): δ 7.65 (d, 1H), 7.54 (d, 1H), 7.45 (d, 2H), 7.31 (s, 3H), 1.98 (t, 4H), 1.66 (qui, 4H), 1.53–1.15 (m, 36H), 0.88 ppm (t, 6H).

9,9-Didodecylfluorene-2-carbaldehyde. To a solution of 2-bromo-9,9-didodecylfluorene (3.5 g, 6.03 mmol) in anhydrous THF (15 mL) was added dropwise *n*-BuLi (2.5 mL, 7.24 mmol) at −78 °C. After stirring for 1 h, anhydrous DMF (2.87 g, 35.0 mmol) was added and stirred for an additional 12 h at 0 °C. The resulting mixture was added to water and extracted with dichloromethane. The organic layer was separated and washed with diluted HCl and then saturated aqueous $NaHCO_3$. The solvent was removed by evaporation and the residue was purified by column chromatography using dichloromethane/petroleum ether (1/10, v/v) as the eluent to give a colorless oil (1.43 g, 45% yield). ^1H NMR (500 MHz, $CDCl_3$): δ 10.05 (s, 1H), 7.85–7.76 (m, 4H), 7.30 (s, 3H), 2.00 (t, 4H), 1.67 (qui, 4H), 1.25–1.12 (m, 36H), 0.87 ppm (t, 6H).

Other 9,9-dialkylfluorene-carbaldehyde intermediates were synthesized as described for 9,9-didodecylfluorene-2-carbaldehyde except that different 1-alkylbromides were used. After purification, they were used without characterization.

9,10-Bis[(9,9-didodecylfluorene-2-yl)vinyl]anthracene (FLA-C12). 9,9-Didodecylfluorene-2-carbaldehyde (0.167 g, 0.46 mmol) and 9,10-bis(diethylphosphorylmethyl)anthracene (0.10 g, 0.21 mmol) were dissolved in 20 mL of anhydrous THF. Potassium *tert*-butoxide (0.19 g, 1.67 mmol) was added and the resulting suspension was stirred for 5 h at room temperature. Methanol was added into the mixture and the resulting solid was collected by filtration. The crude product was purified by silica gel column chromatography (petroleum ether/dichloromethane = 4/1, v/v). After recrystallization from chloroform–methanol, a yellowish-green solid was obtained (0.19 g, 75% yield). ^1H NMR (500 MHz, $CDCl_3$): δ 8.51 (q, 4H), 8.02–7.98 (d, 2H), 7.79–7.23 (m, 18H), 7.06–7.03 (d, 2H), 2.03 (t, 8H), 1.85 (qui, 8H), 1.10–1.25 (m, 72H), 0.85 ppm (t, 12H). ^{13}C NMR (125 MHz, $CDCl_3$): δ 151.51, 151.12, 141.29, 140.77, 138.13, 136.27, 132.83, 129.72, 127.36, 127.09, 126.79, 125.54, 125.18, 124.31, 122.96, 121.04, 119.91, 119.74, 55.11, 53.81, 40.33, 31.86, 30.04, 29.26, 23.83, 22.62, 13.99 ppm (shortage of some alkyl peaks was probably due to peak overlap). Anal. calcd for $C_{92}H_{126}$: C, 89.69; H, 10.31. Found: C, 90.01; H, 10.15%.

Other **FLA-C*n*** derivatives were synthesized and purified as described for **FLA-C12** except that different 9,9-dialkyl-fluorene-2-carbaldehydes were used. Their ^1H NMR, ^{13}C NMR data and elemental analysis were as follows:

FLA-C3: ^1H NMR (500 MHz, $CDCl_3$): δ 8.48 (q, 4H), 8.01–7.98 (d, 2H), 7.79–7.26 (m, 18H), 7.06–7.03 (d, 2H), 2.03 (t, 8H), 1.65 (m, 8H), 0.85 ppm (t, 12H). ^{13}C NMR (125 MHz, $CDCl_3$): δ 151.53, 151.17, 141.32, 140.81, 138.14, 136.37, 132.88, 129.77, 127.52, 127.15, 126.88, 125.54, 125.24, 124.42, 122.55, 121.14, 119.91, 119.74, 55.37, 53.37, 17.31, 14.52 ppm. Anal. calcd for $C_{56}H_{54}$: C, 92.51; H, 7.49. Found: C, 92.12; H, 7.73%.

FLA-C5: ^1H NMR (500 MHz, $CDCl_3$): δ 8.49 (q, 4H), 8.01–7.98 (d, 2H), 7.79–7.26 (m, 18H), 7.06–7.03 (d, 2H), 2.03 (t, 8H), 1.65 (qui, 8H), 1.15–1.09 (m, 16H), 0.75 ppm (t, 12H). ^{13}C NMR (125 MHz, $CDCl_3$): δ 151.53, 151.13, 141.32, 140.81, 138.14, 136.30, 132.86, 129.77, 127.12, 126.88, 126.61, 125.54, 125.24, 124.42, 122.95, 121.02, 119.96, 119.79, 55.14, 53.39, 40.31, 23.49, 22.26, 13.98 ppm. Anal. calcd for $C_{64}H_{70}$: C, 91.59; H, 8.41. Found: C, 91.77; H, 8.52%.

Results and discussion

Synthesis and characterization

FLA-C*n* could be facilely synthesized by the Wittig–Horner reaction of 9,9-dialkylfluorene-2-carbaldehydes (**FL-CHO**) and 9,10-bis(diethoxyphosphorylmethyl)anthracene in high yields of 75–85% (Scheme 1). **FL-CHO** was from the treatment of 2-bromo-9,9-dialkylfluorene with *n*-butyllithium in anhydrous THF followed by the addition of anhydrous DMF. The structure and composition of the target compounds (**FLA-C*n***) were unambiguously characterized by ^1H and ^{13}C NMR and elemental analysis.

Aggregation-induced emission (AIE) in THF–water mixtures

To understand whether a water-nonsoluble conjugated organic molecule is AIE active, a simple and practical method is usually to add a large amount of water into the organic solution of the compound and record the changes of fluorescence intensity.[14,15] **FLA-C*n*** are highly soluble in common organic solvents, such as THF, dichloromethane, chloroform and toluene. Since water is the non-solvent for **FLA-C*n***, the molecules of **FLA-C*n*** must have aggregated in THF–water mixtures with high water content like other 9,10-diarylvinylanthracene derivatives.[10,13,15] The absorption and emission spectra of **FLA-C*n*** in THF–water mixtures are shown in Fig. 1. **FLA-C*n*** are AIE-active with weak fluorescence in molecularly dissolved solution with fluorescence quantum yields (Φ) of 3.8–4.9% but increased fluorescence intensities in aqueous suspensions with Φ of 21–29% at high water content (THF/water = 1/9) (Fig. 1a–c). Because of the large internal steric hindrance between the 1,8-positions of the anthracene ring and the β-positions of the vinylene moieties, the conjugated backbone of 9,10-diaryl-vinylanthracene has been forced to twist strongly.[10i,15a,b] In molecularly dissolved solution, the intramolecular torsion motion is relatively free, which facilitates nonradiative relaxation pathways and affords weak fluorescence emission. However, in aqueous media, the intramolecular vibration and rotation are seriously restricted by molecular self-aggregation, causing the aqueous suspensions to exhibit strongly aggregation-induced emission. On the other hand, there are no significant differences for the absorption spectra of **FLA-C*n*** in solution and aqueous suspension (Fig. 1d). This implies that the molecular stacking in aqueous media is probably loose.

Absorption and emission spectra of pristine FLA-C*n* solids

The fluorescence colors of pristine **FLA-C*n*** solids are gradually blue-shifted with the increase of alkyl length, and **FLA-C3** and

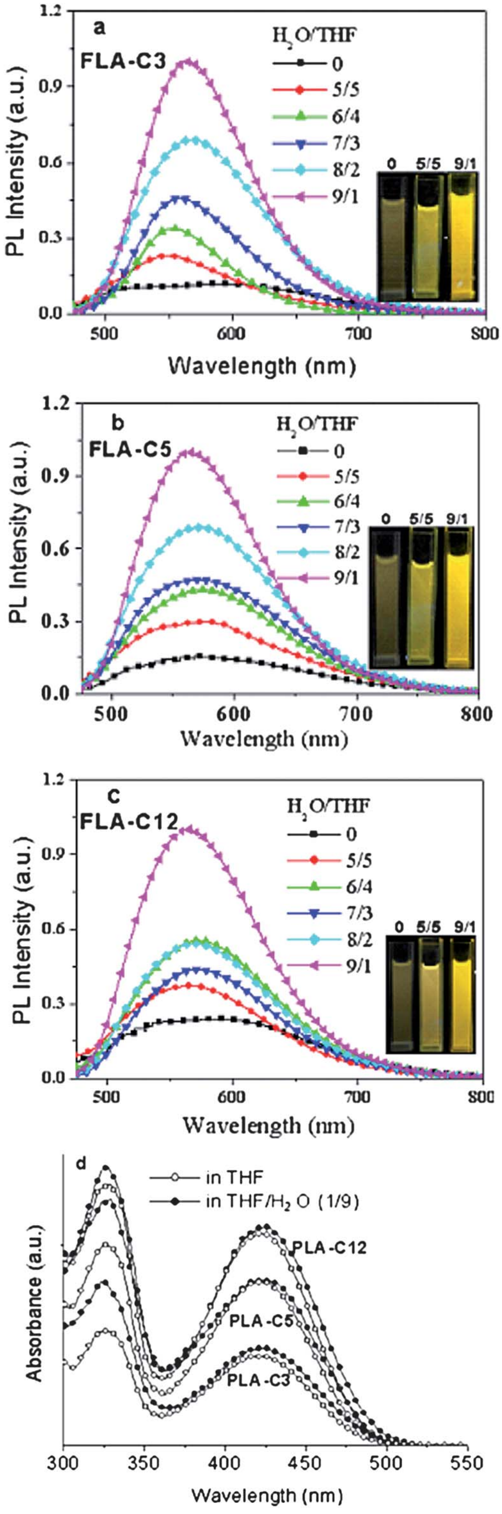

Fig. 1 Emission (PL) spectra (a–c) and absorption spectra (d) of **FLA-C*n*** at 1.0 × 10^{-5} M in water–THF mixtures; the insets are the fluorescence images with water contents of 0%, 50% and 90% under illumination with a 365 nm UV lamp.

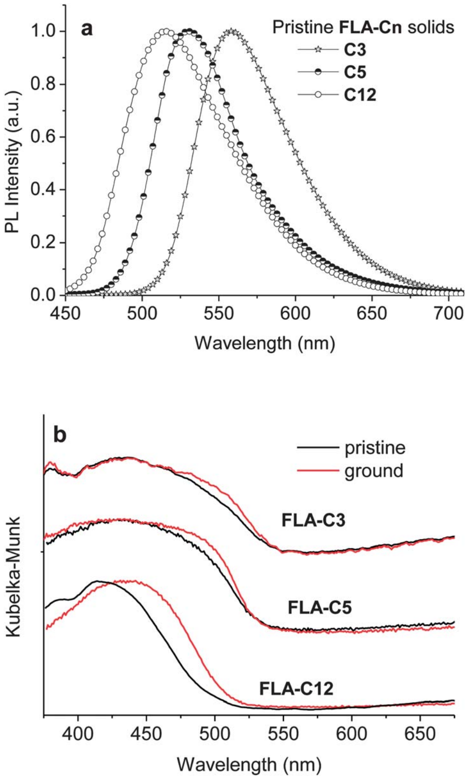

Fig. 2 Fluorescence emission spectra of pristine **FLA-C*n*** solids (a) and diffuse reflectance absorption spectra of pristine and ground **FLA-C*n*** solids (b).

FLA-C12 exhibit yellow (558 nm) and green (515 nm) emission, respectively (Fig. 2a, Table 1). On considering that the only difference between these molecules is the alkyl length, it is concluded that the alkyl chain can affect the solid-state aggregation behavior of **FLA-C*n***. It should be noticed that there have been a variety of reports on the effect of length of alkyl chains on the solid-state aggregation and fluorescence properties of organic fluorophores,[10*i*,13,15*b*,16] however, the reports on the effect of length of alkyl chains on the PFC behaviour are scarce. The chain length-dependent fluorescence properties are believed to be relative to both crystal packing modes (J- or H-aggregation) and the distortion degree of the conjugated backbone.

To understand the different fluorescence emissions of homologous and isomeric fluorophores in crystalline states, an effective and accurate way is to prepare and analyze the single crystal structures. Unfortunately, good-quality single crystals of **FLA-C*n*** could not be obtained probably due to the existence of four side alkyl chains in the twisted backbone, which is unfavorable for the highly ordered alignment of molecules and the formation of high-quality single crystals. Recently, Chi *et al.* have reported that, in the crystalline state, 9,10-bis(*p*-alkoxystyryl)anthracenes (**9,10-DSA**) with long alkyl chains (decyl, undecyl and dodecyl) have more twisted conjugated backbones and weaker intermolecular interactions than those with short alkyl chains (heptyl, octyl and nonyl),[10*i*] which is believed to be the reason why long alkyl-containing **9,10-DSA** derivatives emit shorter PL wavelengths and exhibit larger PFC spectral shifts ($\Delta\lambda_{\mathrm{PFC}}$). We have recently found that shorter alkyl-containing 9,10-bis[(*N*-alkylcarbazol-3-yl)vinyl]anthracenes emit more blue-shifted fluorescence and show larger $\Delta\lambda_{\mathrm{PFC}}$.[13] Thus, it could not be deduced directly that the more blue-shifted fluorescence

Table 1 Peak emission wavelengths (λ, in nm) and thermal transition temperature data of **FLA-Cn** solids under various external stimuli

Cpd	$\lambda_{\text{pristine}}$	λ_{pressed}	$\lambda_{\text{annealed}}$	$\lambda_{\text{repressed}}$	λ_{fumed}	$\Delta\lambda_{\text{PFC}}{}^{a}$	$T_m{}^{b}$/°C	$T_c{}^{c}$/°C
FLA-C3	558	574	556	575	556	18	281	145
FLA-C5	530	554	528	555	532	26	180	132
FLA-C12	514	554	514	552	515	40	65	≤r.t.

[a] $\Delta\lambda_{\text{PFC}} = \lambda_{\text{pressed}} - \lambda_{\text{annealed}}$. [b] Isotropic melt transition temperature. [c] Cold-crystallization temperature of ground **FLA-Cn** solids.

emission of longer alkyl-containing **FLA-C*n*** is due to the more twisted conjugated backbone arising from the long alkyl chains because of the unavailability of crystal structures. Alternatively, we have measured the diffuse reflectance absorption spectra of pristine **FLA-C*n*** solids (black lines, Fig. 2b). It is shown that the absorption spectrum of pristine **FLA-C12** solid is obviously blue-shifted compared with those of pristine **FLA-C3** and **FLA-C5** solids, suggesting a more twisted conjugated backbone for **FLA-C12** than **FLA-C3** and **FLA-C5** in pristine crystals. On the other hand, in comparison with the solution absorption spectra (Fig. 1d), the absorption maximum of **FLA-C12** solid is hypsochromic relative to its solution absorption band, and **FLA-C3** and **FLA-C5** solids show bathochromic absorption maxima relative to their solutions. In view of these absorption spectra, **FLA-C12** may be H-aggregates though it has strong fluorescence,[15b] and **FLA-C3** and **FLA-C5** are possibly J-aggregates. This deduction is also supported partly by the more blue-shifted emission for **FLA-C12** than **FLA-C3** and **FLA-C5** solids (Fig. 2a).

Solid-state piezochromic luminescence

We have examined the PFC behaviour of **FLA-C*n*** solids (mixed with KBr to minimize the amount of fluorophores) by pressing with an IR pellet press (30 seconds at 1500 psi). Pristine **FLA-C12, FLA-C5** and **FLA-C3** solids emit green, yellowish-green and yellow fluorescence, respectively. However, when they are pressed, **FLA-C12** and **FLA-C5** are changed into yellow-emitting solids and **FLA-C3** becomes yellowish-orange emitting (left column, Fig. 3). Moreover, when the pressed samples are annealed before the isotropic melt transition or exposed to solvent vapor (fuming above dichloromethane), the fluorescence colors are recovered to the original ones. Furthermore, when the fumed or annealed samples are re-pressed, the fluorescence colors are again changed as the first pressing. This process is very reproducible and indicates reversible PFC behaviour. It is noted that the longer the alkyl chain of **FLA-C*n***, the more remarkable the fluorescence color change upon pressing (Fig. 3).

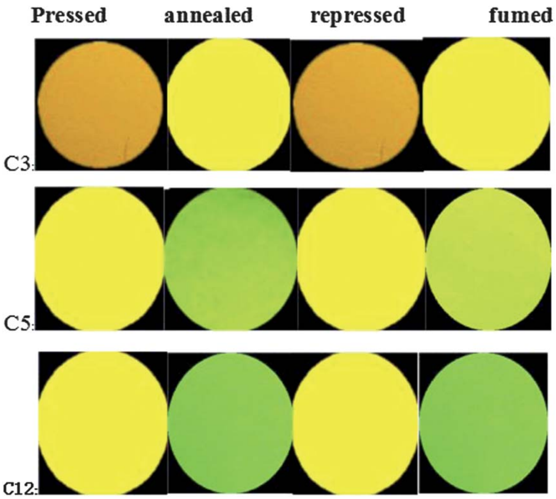

Fig. 3 Fluorescence images of **FLA-C*n*** solids mixed with KBr upon pressing and annealing under a 365 nm UV lamp.

These naked-eye-visible fluorescence color changes were recorded on a luminescence spectrophotometer. The spectral data are summarized in Table 1, and the emission spectra of pressed and annealed **FLA-C*n*** samples are depicted in Fig. 4. It can be seen that the emission spectra are very consistent with the corresponding fluorescence colors observed (Fig. 3). The pressing-induced spectral shifts ($\Delta\lambda_{\text{PFC}} = \lambda_{\text{pressed}} - \lambda_{\text{annealed}}$) of **FLA-C12**, **FLA-C5** and **FLA-C3** solids are 40, 26, and 18 nm, respectively. This implies that **FLA-C*n*** solids are also chain length-dependent PFC materials, and alkyl chains have played a functional role in tuning the PFC behavior of **FLA-C*n*** although such alkyl elements are normally inactive and undesirable for optoelectronic properties. It is noted that the alkyl length-dependent PFC behaviour of **FLA-C*n*** is similar to those of 9,10-bis(*p*-dialkoxylstyryl)anthracenes[10i] and β-cyano-substituted bis(*p*-alkoxystyryl)benzenes[5a] but thoroughly different from that of 9,10-bis[(*N*-alkylcarbazol-3-yl)vinyl]anthracenes.[13] The origin for this dichotomous alkyl chain length-dependent PFC behaviour is not clear at present, underlining the complexity of the structure–property relationship of PFC materials.

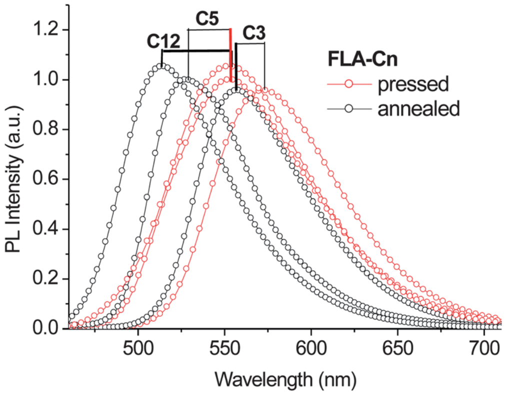

Fig. 4 Emission spectra of **FLA-C*n*** solids mixed with KBr upon pressing and annealing.

Another interesting phenomenon is the PFC behaviour of pure **FLA-C12** solid. Just ground **FLA-C12** solid emits yellow fluorescence, however, when it is left standing at room temperature, the fluorescence colour changes with the increase of standing time and gradually recovers to the original green emission (Fig. 5, top). The lower part of Fig. 5 is the change curve of the peak emission wavelength of ground **FLA-C12** solid *versus* the standing time. It is shown that the rapid recovering in fluorescence colour and emission happens within the initial 10 min (form 553 to 522 nm), and standing for 60 min, the fluorescence emission (515 nm) is almost identical with the pristine solid (514 nm) and almost unchanged further. In view of the changes in fluorescence colour and emission spectra, grinding has the same effect as pressing. On the other hand, unlike **FLA-C12**, the fluorescence colours and emission spectra of ground **FLA-C3** and **FLA-C5** solids remain orange and yellow over 24 h at room temperature. These findings suggest that we can endow 9,10-diarylvinyl-anthracene dyes with stable or self-recovering PFC behaviour by altering the end-arylenes and tuning the alkyl length. PFC materials with tunable recovering behaviour could be useful for various applications.

X-ray diffraction and DSC analysis

To gain an insight into the PFC behaviour of **FLA-C*n*** solids, powder wide-angle X-ray diffraction (PXD) and differential scanning calorimetry (DSC) experiments were conducted on the ground and pristine solids. The PXD patterns of pristine **FLA-C3** and **FLA-C5** solids show sharp and intense reflections, indicative of their well-ordered microcrystalline structures (Fig. 6a). In contrast, the ground samples display broad and featureless diffractograms reflecting notable amorphous features. This indicates that grinding has induced the phase transition of **FLA-C*n*** solids between crystalline and amorphous states, which should be responsible for the PFC behaviour of **FLA-C*n*** solids. The formation of amorphous state upon grinding was also confirmed by DSC experiments. As shown in Fig. 6b, no additional thermal transitions could be detected for all pristine solids before the isotropic melt transition (T_m); however, there is clearly one exothermic transition peak at the lower-temperature region for ground **FLA-C3** and **FLA-C5** solids. This broad exothermic peak (T_c) is ascribed to the cold-crystallization of amorphized **FLA-C*n*** solids upon heating. Amorphized **FLA-C3** and **FLA-C5** solids have high T_c values, which result in their stable PFC behaviour at room temperature. It is known that the T_c is obviously lower than the T_m of a compound, and the ground **FLA-C12** solid could cold-crystallize at or below room temperature since its isotropic melt point is only about 65 °C. Thus, the amorphized **FLA-C12** solid induced by grinding is in a thermodynamically and dynamically unstable morphology. This is reason why ground **FLA-C12** solid exhibits spontaneously recovering fluorescence properties at room temperature.

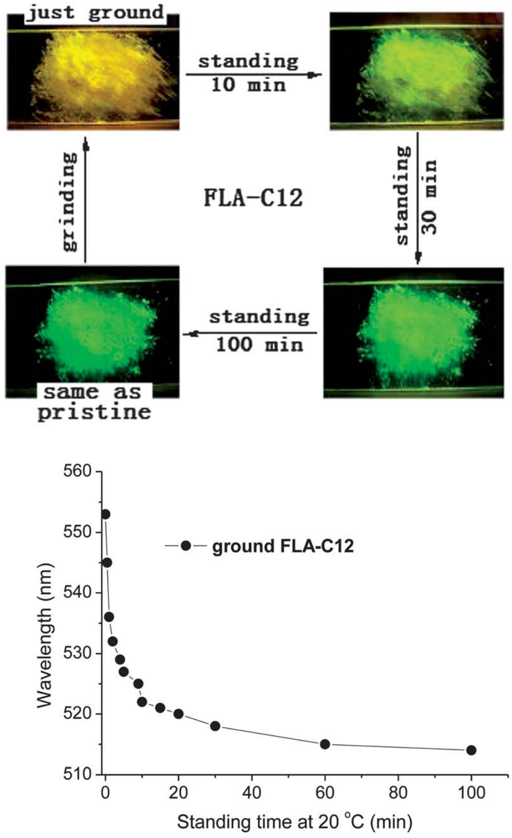

Fig. 5 Fluorescence images (upper) and the peak emission wavelengths (lower) of ground pure **FLA-C12** solid at different standing times at room temperature.

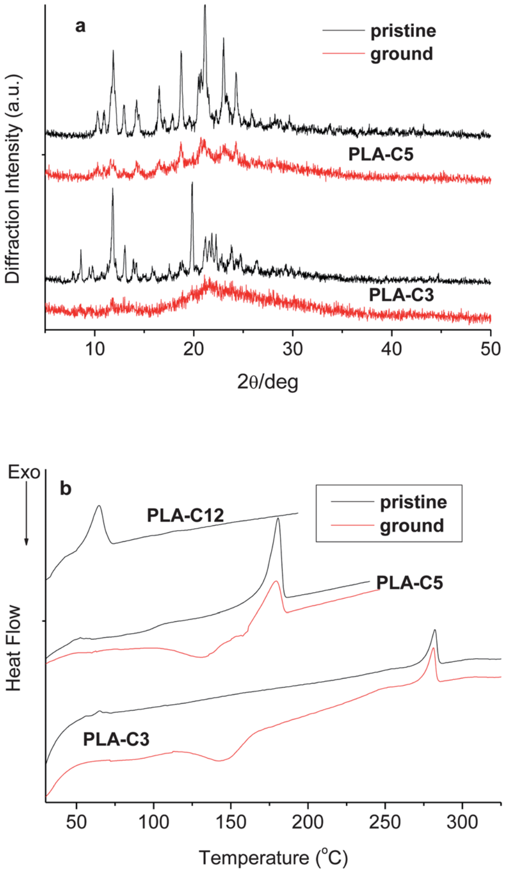

Fig. 6 Powder X-ray diffraction patterns at room temperature (a) and DSC curves (b) of ground and pristine **FLA-C*n*** solids.

To understand the chain length-dependent PFC behaviour of **FLA-C*n***, the diffuse reflectance absorption spectra of ground samples were recorded (red lines, Fig. 2b). It is observed that grinding does not significantly affect the absorption maxima of **FLA-C3** and **FLA-C5**; however, the absorption maximum of **FLA-C12** is obviously red-shifted by grinding. Thus, it could be considered that the conjugated backbone of **FLA-C12** becomes less twisted upon grinding. Since the conjugated backbone of **FLA-C12** in pristine crystal is probably more twisted (*vide supra*) and the intermolecular interactions are weaker (low T_c), grinding could not only destroy easily the crystal structure of **FLA-C12** but also induce the backbone conformation to change largely, resulting in a large $\Delta\lambda_{PFC}$. The real origin for this unique chain length-dependent PFC behaviour is still under investigation in our laboratory. Finally, it is noticed that the fluorescence color of the pressed **FLA-C12** sample diluted with KBr is more stable and can remain unchanged over 5 min at room temperature. This implies that KBr could reduce the molecular motion and delay the cold-crystallization rate of **FLA-C*n***. This is also an interesting phenomenon that requires investigation.

Conclusions

We have demonstrated new alkyl length-dependent solid-state fluorescence and piezochromic luminescence properties of AIE-active 9,10-bis[(9,9-dialkylfluorene-2-yl)vinyl]anthracenes (**FLA-C*n***) with propyl, pentyl and dodecyl side chains. The fluorescence emissions of pristine **FLA-C*n*** solids are blue-shifted with the increase of the length of alkyl chains and the spectral shifts induced by pressing are increased with the length of alkyl chains. This is thoroughly different from the behaviour observed previously in 9,10-bis[(*N*-alkyl-carbazol-3-yl)vinyl] anthracenes, implying that both the nature of end-arylenes capped at divinylanthracene and the substituents on the aryl rings have important effects on the solid-sate fluorescence and piezochromic luminescence of 9,10-diarylvinylanthracene derivatives. PXD and DSC reveal that the transformation between crystalline and amorphous states upon various external stimuli is responsible for the PFC behavior. We have also observed an intriguing PFC behaviour that the fluorescence emission of ground **FLA-C12** solid can recover spontaneously at room temperature, which is ascribed to the low cold-crystallization temperature of amorphized **FLA-C12** solid. This work has demonstrated once again that the subtle manipulation of end groups of 9,10-diarylvinylanthracenes could endow them with unique and tunable solid-state optical properties.

Acknowledgements

We thank the NSFC of China (no. 51173092, 51073083), NSF of Shandong Province (no. ZR2010EM023, ZR2012-EMQ003), and Open Project of State Key Laboratory of Supramolecular Structure and Materials of Jilin University (no. SKLSSM201310).

Notes and references

1 Y. Sagara and T. Kato, *Nat. Chem.*, 2009, **1**, 605.

2 C. Weder, Editorial, *J. Mater. Chem.*, 2011, **21**, 8235.

3 Z. Chi, X. Zhang, B. Xu, X. Zhou, C. Ma, Y. Zhang, S. Liu and J. Xu, *Chem. Soc. Rev.*, 2012, **41**, 3878.

4 J. W. Chung, Y. You, H. S. Huh, B. K. An, S. J. Yoon, S. H. Kim, S. W. Lee and S. Y. Park, *J. Am. Chem. Soc.*, 2009, **131**, 8163.

5 (*a*) J. Kunzalman, M. Kinami, B. R. Crenshaw, J. D. Protasiewicz and C. Weder, *Adv. Mater.*, 2008, **20**, 119; (*b*) H. Ito, T. Saito, N. Oshima, N. Kitamura, S. Ishizaka, Y. Hinatsu, M. Wakeshima, M. Kato, K. Tsuge and M. Sawamura, *J. Am. Chem. Soc.*, 2008, **130**, 10044; (*c*) A. L. Balch, *Angew. Chem., Int. Ed.*, 2009, **48**, 2.

6 (*a*) T. Tsukuda, M. Kawase, A. Dairiki, K. Matsumoto and T. Tsubomura, *Chem. Commun.*, 2010, **46**, 1905; (*b*) B.-C. Tzeng, T.-Y. Cheng and H.-S. Sheu, *Chem.–Eur. J.*, 2010, **16**, 9990; (*c*) S. Perruchas, X. F. Le Goff, S. Maron, I. Maurin, F. Guillen, A. Garcia, T. Gacoin and J.-P. Boilot, *J. Am. Chem. Soc.*, 2010, **132**, 10967; (*d*) G. Zhang, J. Lu, M. Sabat and C. L. Fraser, *J. Am. Chem. Soc.*, 2010, **132**, 2160; (*e*) Z. Zhang, D. Yao, T. Zhou, H. Zhang and Y. Wang, *Chem. Commun.*, 2011, **47**, 7782.

7 (*a*) Y. Ooyama, Y. Kagawa, H. Fukuoka, G. Ito and Y. Harima, *Eur. J. Org. Chem.*, 2009, 5321; (*b*) Y. Ooyama, G. Ito, H. Fukuoka, T. Nagano, Y. Kagawa, I. Imae, K. Komaguchi and Y. Harima, *Tetrahedron*, 2010, **66**, 7268; (*c*) Y. Ooyama and Y. Harima, *J. Mater. Chem.*, 2011, **21**, 8372; (*d*) Y. Ooyama, N. Yamaguchi, S. Inoue, T. Nagano, E. Miyazaki, H. Fukuoka, I. Imae, K. Komaguchi, J. Ohshita and Y. Harima, *Tetrahedron*, 2012, **68**, 529–533.

8 (*a*) K. Mizuguchi and H. Nakano, *Dyes Pigm.*, 2013, **96**, 76; (*b*) J. Liang, F. Hu, X. Lv, Z. Chen, Z. Chen, J. Yin, G.-A. Yu and S. Hua, *Dyes Pigm.*, 2012, **95**, 485; (*c*) K. Mizuguchi, H. Kageyama and H. Nakano, *Mater. Lett.*, 2011, **65**, 2658.

9 (*a*) S.-J. Yoon, J. W. Chung, J. Gierschner, K. S. Kim, M.-G. Choi, D. Kim and S. Y. Park, *J. Am. Chem. Soc.*, 2010, **132**, 13675; (*b*) S. J. Yoon and S. Y. Park, *J. Mater. Chem.*, 2011, **21**, 8338.

10 (*a*) B. Xu, Z. Chi, J. Zhang, X. Zhang, H. Li, X. Li, S. Liu, Y. Zhang and J. Xu, *Chem.–Asian J.*, 2011, **6**, 1470; (*b*) X. Zhou, H. Li, Z. Chi, X. Zhang, J. Zhang, B. Xu, Y. Zhang, S. Liu and J. Xu, *New J. Chem.*, 2012, **36**, 685; (*c*) B. Xu, Z. Chi, X. Zhang, H. Li, C. Chen, S. Liu, Y. Zhang and J. Xu, *Chem. Commun.*, 2011, **47**, 11080; (*d*) X. Zhang, Z. Chi, H. Li, B. Xu, X. Li, W. Zhou, S. Liu, Y. Zhang and J. Xu, *Chem.–Asian J.*, 2011, **6**, 808; (*e*) H. Li, X. Zhang, Z. Chi, B. Xu, W. Zhou, S. Liu, Y. Zhang and J. Xu, *Org. Lett.*, 2011, **13**, 556; (*f*) H. Li, Z. Chi, B. Xu, X. Zhang, X. Li, S. Liu, Y. Zhang and J. Xu, *J. Mater. Chem.*, 2011, **21**, 3760; (*g*) X. Zhang, Z. Chi, J. Zhang, H. Li, B. Xu, X. Li, S. Liu, Y. Zhang and J. Xu, *J. Phys. Chem. B*, 2011, **115**, 7606; (*h*) X. Zhang, Z. Chi, B. Xu, C. Chen, X. Zhou, Y. Zhang, S. Liu and J. Xu, *J. Mater. Chem.*, 2012, **22**, 18505; (*i*) X. Zhang, Z. Chi, B. Xu, L. Jiang, X. Zhou, Y. Zhang, S. Liu and J. Xu, *Chem. Commun.*, 2012, **48**, 10895.

11 X. Luo, J. Li, C. Li, L. Heng, Y. Q. Dong, Z. Liu, Z. Bo and B. Z. Tang, *Adv. Mater.*, 2011, **23**, 3261.

12 Y. Dong, B. Xu, J. Zhang, X. Tan, L. Wang, J. Chen, H. Lv, S. Wen, B. Li, L. Ye, B. Zou and W. Tian, *Angew. Chem., Int. Ed.*, 2012, **51**, 10782–10785.

13 Y. Wang, W. Liu, L. Bu, J. Li, M. Zheng, D. Zhang, M. Sun, Y. Tao, S. Xue and W. Yang, *J. Mater. Chem. C*, 2013, **1**, 856.

14 (*a*) J. Luo, Z. Xie, J. W. Y. Lam, L. Cheng, H. Chen, C. Qiu, H. S. Kwok, X. Zhan, Y. Liu, D. Zhu and B. Z. Tang, *Chem. Commun.*, 2001, 1740; (*b*) B.-K. An, S.-K. Kwon, S.-D. Jung and S. Y. Park, *J. Am. Chem. Soc.*, 2002, **124**, 14410; (*c*) Y. Hong, J. W. Y. Lam and B. Z. Tang, *Chem. Commun.*, 2009, 4332; (*d*) Y. Hong, J. W. Y. Lam and B. Z. Tang, *Chem. Soc. Rev.*, 2011, **40**, 5361.

15 (*a*) J. He, B. Xu, F. Chen, H. Xia, K. Li, L. Ye and W. Tian, *J. Phys. Chem. C*, 2009, **113**, 9892; (*b*) Y. Wang, T. Liu, L. Bu, J. Li, C. Yang, X. Li, Y. Tao and W. Yang, *J. Phys. Chem. C*, 2012, **116**, 15576; (*c*) H. Lu, B. Xu, Y. Dong, F. Chen, Y. Li, Z. Li, J. He, H. Li and W. Tian, *Langmuir*, 2010, **26**, 6838; (*d*) B. Xu, J. He, Y. Dong, F. Chen, W. Yu and W. Tian, *Chem. Commun.*, 2011, **47**, 6602; (*e*) S. Kim, Q. Zheng, G. S. He, D. J. Bharali, H. E. Pudavar, A. Baev and P. N. Prasad, *Adv. Funct. Mater.*, 2006, **16**, 2317.

16 (*a*) R. Thomas, S. Varghese and G. U. Kulkarni, *J. Mater. Chem.*, 2009, **19**, 4401; (*b*) R. Davis, N. P. Rath and S. Das, *Chem. Commun.*, 2004, 74; (*c*) N. S. S. Kumar, S. Varghese, C. H. Suresh, N. P. Rath and S. Das, *J. Phys. Chem. C*, 2009, **113**, 11927; (*d*) R. Davis, N. S. S. Kumar, S. Abraham, C. H. Suresh, N. P. Rath, N. Tamaoki and S. Das, *J. Phys. Chem. C*, 2008, **112**, 2137; (*e*) N. S. S. Kumar, S. Varghese, N. P. Rath and S. Das, *J. Phys. Chem. C*, 2008, **112**, 8429.